Check for
updates

Gracilariopsis lemaneiformis Polysaccharide Attenuates D-Galactose–Induced Aging of Mice by Regulating Oxidative Stress and Gut Microbiota

Zhongshan Zhang[1]*, Xinyue Li[1], Xiaogang Xu[2], Genxiang Mao[2], Xue Sun[3], Nianjun Xu[3]* and Xiaomei Wang[1]*

[1] Key Laboratory of Vector Biology and Pathogen Control of Zhejiang Province, Huzhou University, Huzhou, China, [2] Key Lab of Geriatrics and Geriatrics Institute of Zhejiang Province, Department of Geriatrics, Zhejiang Hospital, Hangzhou, China, [3] National Engineering Research Laboratory of marine biotechnology and Engineering, Key Laboratory of Marine Biotechnology of Zhejiang Province, School of Marine Sciences, Ningbo University, Ningbo, China

Gracilariopsis lemaneiformis polysaccharide (GP) exerted protective effects in an aging mouse model administered with D-galactose, and its mechanism was revealed. GP increased the activity of antioxidant enzymes, reduced malondialdehyde levels in the brain and serum, alleviated D-galactose–induced damage to the liver, and ameliorated mild cognitive impairment. Abundance of the gut microbiota differed significantly between GP and control groups. GP alleviated liver and brain injuries by regulating oxidative stress and modulating the composition and metabolism of the gut microbiota.

Keywords: G. lemaneiformis, polysaccharide, aging, oxidative stress, gut microbiota

INTRODUCTION

Aging is an inevitable and multifactorial process characterized by progressive decline in antioxidant function and subsequence increase in oxidative damage caused by reactive oxygen species and other oxidation products (Forman, 2016; Galkin et al., 2019). Therefore, research on prevention of aging, treatment of aging-related diseases, and improvement of vitality and quality of life is underway. Chronic systemic administration of D-galactose in animal models could artificially mimic human brain senescence, manifesting as characteristic features of natural aging, such as cognitive deficit and nervous system damage (Xu et al., 2016; Rehman et al., 2017). In addition, activities of antioxidant enzymes, such as glutathione peroxidase (GSH-Px) and superoxide dismutase (SOD) decreased in tissues. Therefore, D–galactose–treated mice have been widely regarded as an ideal aging-related animal model to study pharmacological interventions for cognitive decline (Cui et al., 2006).

Intestinal flora changes significantly with aging and related diseases (Lakshminarayanan et al., 2014). Reduced abundance of the beneficial gut microbiome with aging decreases the level of

corresponding microbial metabolites, such as short-chain fatty acids (García-Pea et al., 2017). Therefore, proliferating the beneficial gut microbiome is a novel strategy to reduce systemic inflammation, improve intestinal barrier function, reduce senile diseases, and prolong a healthy life.

Carbohydrates are widely distributed in animals, plants, and microorganisms. In addition to being components of animal and plant cell walls and nutrients stored in tissues, many carbohydrates perform special biological activities and have been widely used in food, chemicals, medicines, health products, and so on (Yosri et al., 2021). Many polysaccharides from marine organisms perform excellent anti-aging activities (Wang et al., 2021). Their antioxidant and immune-boosting properties exert anti-aging effects. Red algae *Gracilariopsis lemaneiformis* polysaccharide (GP) extends the adult lifespans of wild-type and polyQ nematodes through the insulin pathway DAF-16 (Wang et al., 2019). The aim of this study was to investigate the anti-aging effects of GP in humans from the perspective of serum metabolomics and intestinal microorganisms using a mouse aging model subcutaneously injected with D-galactose.

MATERIALS AND METHODS

Samples
GP were extracted from red algae *G. lemaneiformis* with citric acid as a solvent, as described previously (Wang et al., 2018). The powder was dissolved in normal saline as a working solution. D-galactose was purchased from Sigma-Aldrich (St. Louis, MO, USA). The kits for estimating the related indicator content were purchased from Nanjing Jiancheng Biochemical Co., Ltd.

Animals and Treatments
Forty-two female Kunming mice, weighing 18–20 g, were purchased from Shanghai SLAC Laboratory Animal Co., Ltd. (Shanghai, China). They were housed at room temperature under 40%–60% humidity and maintained under a 12-h light/dark cycle with free access to food and water. After 1 week of adaptation to the environment, the mice were randomly assigned to the following six groups (10 per group): control group, daily treated with an intraperitoneal injection of saline (0.9% NaCl); D-galactose group, daily treated with an intraperitoneal injection of D-galactose (120 mg/kg) for 8 weeks; positive control group, daily treated with an intragastric injection of aminoguanidine (100 mg/kg/day); and GP groups, daily treated with an intraperitoneal injection of D-galactose (120 mg/kg) for 8 weeks and divided into the low-, medium-, and high-dose subgroups with oral administration of GP at 125, 250, and 500 mg/kg/day, respectively.

Morris Water Maze Test
The mice were evaluated in the Morris water maze for learning and memory abilities. They were trained in a circular pool (80 × 30 cm) and an escape platform (10 × 25 cm). The circular pool was filled with opaque water (25 ± 3°C) rendered by ink, and the escape platform was submerged 1–2 cm below the water surface. The first 5 days were the training period, and the last day was the testing

period. For 30 min before the experiment, the mice in each group were put in the corresponding room to fully adapt to the environment. During the training period, each mouse practiced thrice a day, and the next training was carried out at a certain interval. First, the mice were held in hands such that they faced the pool wall and then randomly placed in water. They were submerged in the pool from all four directions with the head near the pool wall. Time taken by the mice to search and board the platform was recorded after a latency period of 60 s. If the mice could not find the platform successfully, they were guided to find it and placed on the platform for 30 s. On the last day, the incubation period of all mice was tested and recorded.

Serum and Tissue Preparation
At the end of the test, approximately 0.5 g of fresh mice feces were collected and stored in a sterilized test tube at −80°C. Blood was collected by removing the eyeball 12 h after the final administration, stored for 30 min, and then centrifuged for 10 min until the supernatant was obtained as serum. The serum samples were stored at −20°C. Each hippocampus tissue was weighed, homogenized with cold saline, and centrifuged to obtain the supernatant for further experiments. After drawing blood, the mice were killed, and the liver, spleen, and thymus tissues were excised on ice. The dorsal skin samples (approximately 7 mm × 7 mm) were removed, degreased with 1:1 acetone ether, and transferred into the cryopreservation tube for use.

Biochemical Analysis
Thymus and spleen weights were divided by the maternal body weight to obtain thymus and spleen indices. Serum and hippocampus homogenates were used to detect SOD, CAT, and GSH-Px activities and malondialdehyde levels. Interleukin-2, interleukin-6, and advanced glycation end-products (AGEs) in the hippocampus were detected using the kit. Hydroxyproline content in skin was measured using the hydroxyproline assay kit according to the manufacturer's instructions.

The liver tissue from the fixed solution was embedded in a paraffin block. The block was fixed in a slicer and cut into thin slices. After dewaxing, the slices were stained with hematoxylin-eosin staining, dehydrated, sealed, and examined under a microscope. Finally, images were collected and analyzed.

Gut Microbial Sequencing of Fecal Samples
Total genome DNA from fecal samples was extracted using the TIANamp Soil DNA Kit (TIANGEN Biotech Co., Ltd., Beijing, China). In addition, 16S ribosomal RNA gene sequencing was performed by Wekemo Tech Group Co., Ltd. (Shenzhen, China), as described previously (Zhang et al., 2018).

Statistical Analysis
Data are expressed as mean ± standard deviation. A *P*-value of <0.05 was considered to be statistically significant. Between-group differences were evaluated by the one-way analysis of variance followed by Duncan's multiple range tests.

RESULTS

Chemistry of GP

The chemical composition and related structural information of GP have been published previously (Wang et al., 2018). In brief, GP have 97.59% purity. A monosaccharide compositional analysis revealed that GP contained abundant galactose and relatively less glucose. GP are linear and contain alternating α-(1→3)– and β-(1→4)–galactopyranose units. Most sulfate groups are at C6 of the –(1→4)-α-D-Galp, and some sulfate groups are etherified at C3 and C6.

General Status and Organ Index of the Mice

During the whole experiment, mice body weight did not differ among groups. However, both positive control and GP groups showed reversed symptoms of activity attenuation and reduced vigor and hair loss induced by D-galactose. Compared with the D-galactose group, mice in the other groups showed relatively bright hair and flexible exercise ability.
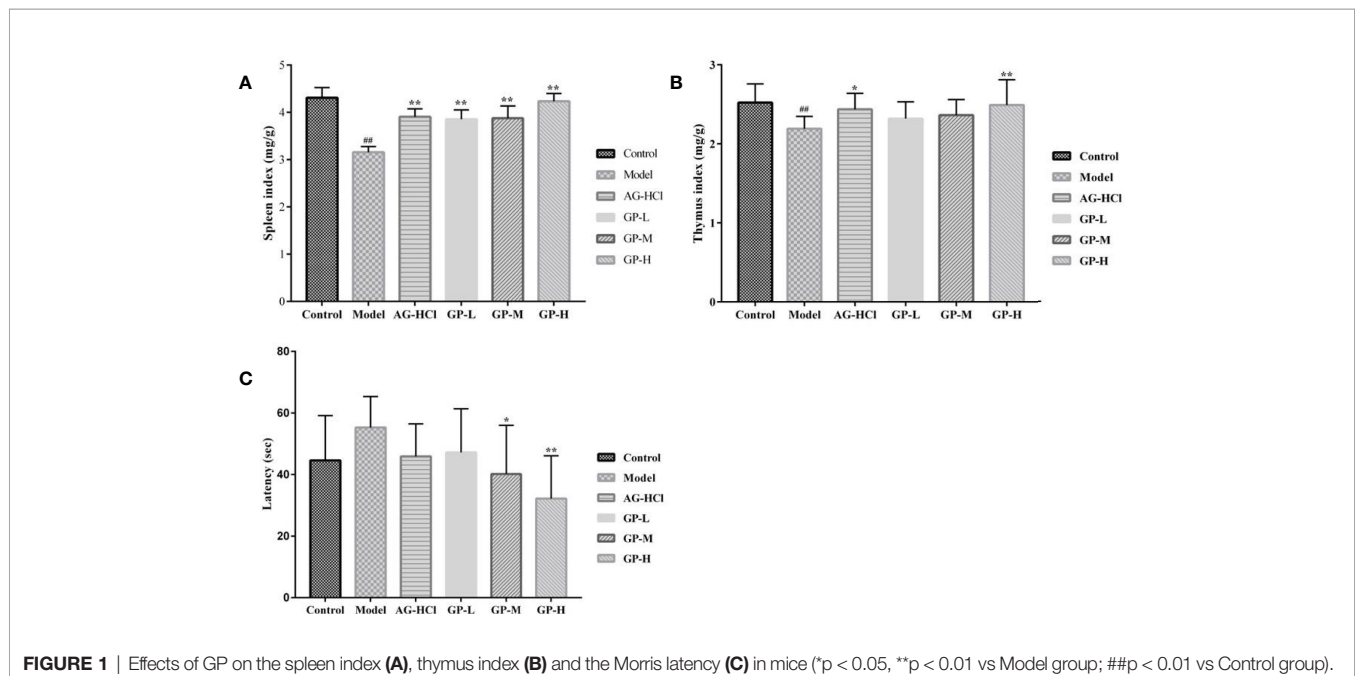
Aging is associated with decline in immune function, and the spleen index reflects the immune function of the spleen. D-galactose causes the accumulation of reactive oxygen species, which the spleen and thymus are susceptible to (Borgoni et al., 2021). Compared with the control group, organ index scores of the spleen and thymus were significantly reduced in the D-galactose group ($P < 0.01$; **Figure 1**). In contrast, compared with the D-galactose group, treatment with GP at low and medium doses improved the liver index of aging mice, although without significant difference ($P > 0.05$), with high doses exhibiting the highest value among the groups ($P < 0.01$). Treatment with GP at low, medium, and high doses significantly increased the thymus index ($P < 0.01$) by 34.18%, 22.81%, and 22.15%, respectively.

Learning and Memory Abilities Of Mice

The Morris water maze test is based on the survival instinct of animals to find an escape platform. The process of finding the escape platform involves collecting memories related to spatial positioning. The mice in the D-galactose group spent more time in latency to find the platform than those in the control group (**Figure 1**). They had poor balance ability in water, and their bodies tilted and choked seriously. Most mice in the D-galactose group could not find the platform within 60 s, indicating severe memory decline. The decline in spatial positioning memory based on vision hindered the mice from recalling the platform position or rendered an unclear memory. Therefore, they blindly searched for the escape path or turned around at the pool wall every time. However, treatment with high and medium doses of GP was associated with significantly less time spent in latency ($P < 0.05$ and $P < 0.01$, respectively). Treatment with GP at a low dose or aminoguanidine shortened the escape latency although without statistical significance ($P > 0.05$). Thus, GP reversed the spatial cognition and learning decline caused by D-galactose.

Histopathology of Liver Tissues

The anatomical results showed that the liver of mice in the control group was brownish red, with a sharp edge, smooth surface, tough texture, and normal appearance. In contrast, the liver color was slightly lighter in the D-galactose group than in the control group, without white necrosis points. Compared with the D-galactose group, the liver color in the GP group appeared red and normal. **Figure 2** shows the hematoxylin-eosin staining results of the liver in each group. In the control group, the liver tissues showed ubiquitous polygonal hepatocytes, minor binucleation of hepatocytes, and radially arranged hepatic cords around a central vein. However, hepatocytes were disordered and arranged loosely, and the number of inflammatory cells and
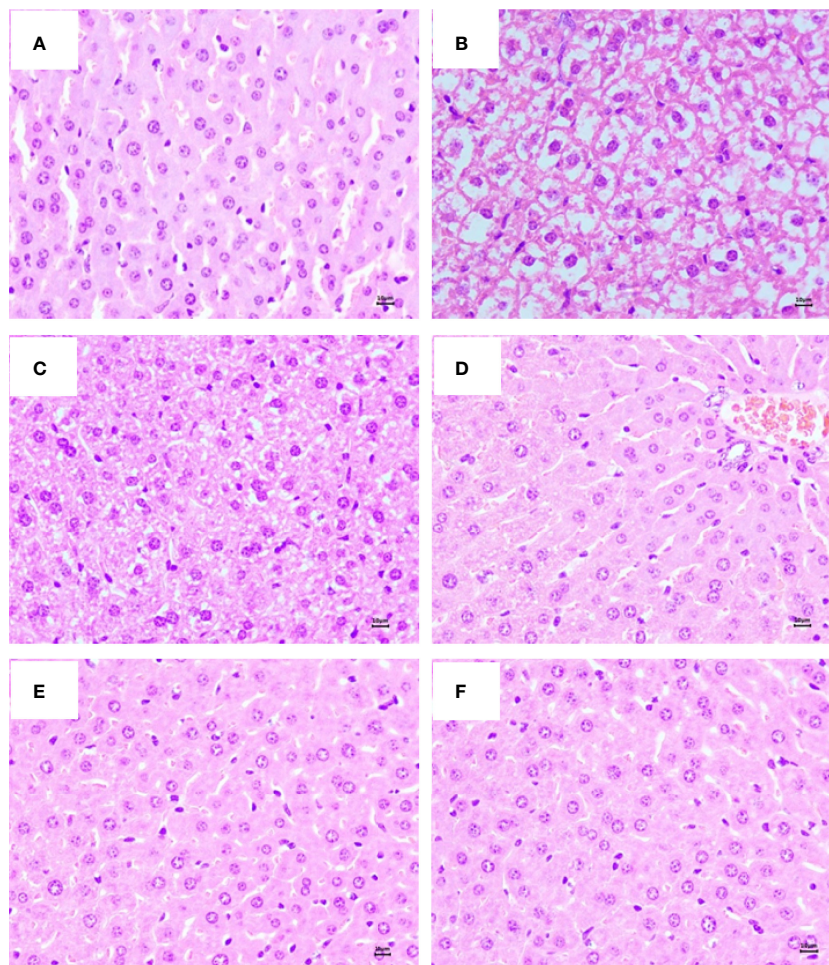

FIGURE 1 | Effects of GP on the spleen index **(A)**, thymus index **(B)** and the Morris latency **(C)** in mice (*p < 0.05, **p < 0.01 vs Model group; ##p < 0.01 vs Control group).

FIGURE 2 | Representative photography (hematoxylin and eosin, HE, mangnification,×40, 10 μm) staining of liver in mice. **(A)** Control group; **(B)** Model group; **(C)** AG-HCl group. **(D)** GP-L group. **(E)** GP-M group. **(F)** GP-H group.

vacuoles increased in the D-galactose group. Co-treatment of D-galactose with GP or aminoguanidine improved these situations. Particularly, hepatocytes in the GP group were clearly visible and arranged neatly, similar to the control group.

Oxidative Stress and Inflammatory Factors

Oxidative stress is a common stimulating factor associated with aging (Ionescu-Tucker and Cotman, 2021). Therefore, these indices in serum and brain were analyzed to determine the degrees of oxidative damage. Mice serum and brain in the D-galactose group showed remarkably lower activities of SOD, CAT, and GSH-Px and elevated malondialdehyde compared with the control group ($p < 0.01$; **Figures 3**, **4**). Treatment with GP could markedly restore or decrease these reactive oxygen species-scavenging antioxidant enzymes in direct correlation to the dose. Significant effects also occurred in the aminoguanidine group.

Immunosenescence-related inflammation in aging is mainly characterized by upregulation of pro-inflammatory cytokines (such as interleukin-6) and downregulation of anti-inflammatory cytokines (such as interleukin-2) (Sendama, 2020). Interleukin-2 levels in the D-galactose group were significantly decreased ($P < 0.01$) and interleukin-6 levels significantly increased ($P < 0.01$) compared with the control group (**Figure 5**). In contrast, treatment with GP significantly increased interleukin-2 levels and decreased interleukin-6 levels compared with the D-galactose group ($P < 0.05$ and $P < 0.01$, respectively). Thus, GP suppressed the expression of hippocampal inflammatory cytokines in aging mice.

Level of AGEs and Hydroxyproline

Formation of AGEs is closely associated with physicochemical changes in connective tissue with aging (Vlassara, 1997). Inhibition of AGE formation in age-related chronic diseases may limit oxidative and inflammatory damages in tissues, retarding the progression of pathophysiology and improving the quality of life during aging (Baynes, 2001). Therefore, it can be used as an important index to study aging. Brain levels of AGEs in the D-galactose group were significantly higher ($P < 0.01$) compared with
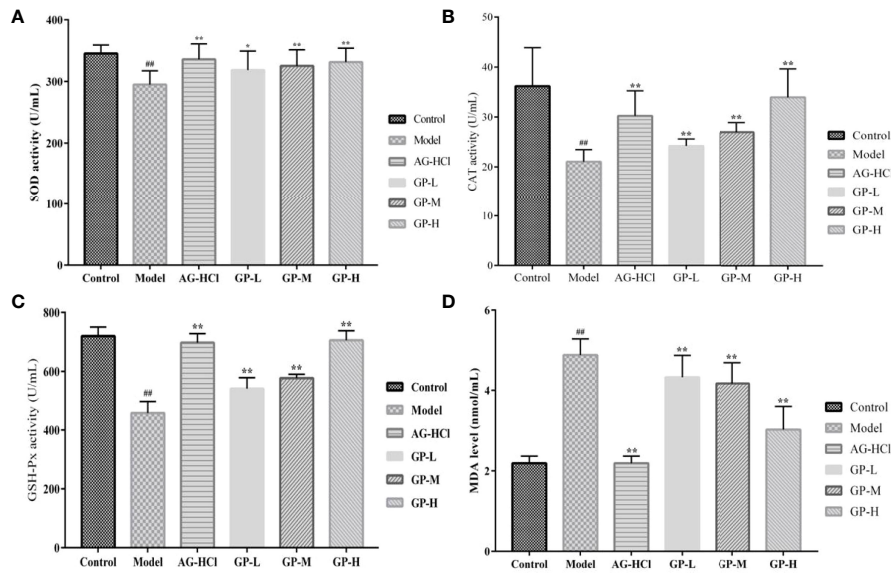
FIGURE 3 | Effects of GP on SOD **(A)**, GSH-Px **(B)**, CAT **(C)**, and MDA **(D)** in serum of mice (*p < 0.05, **p < 0.01 vs Model group; ##p < 0.01 vs Control group).
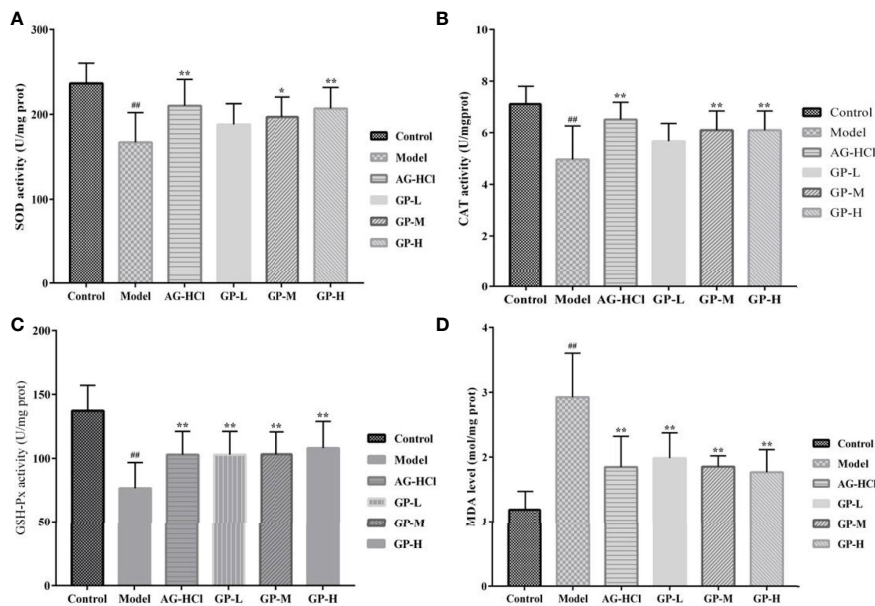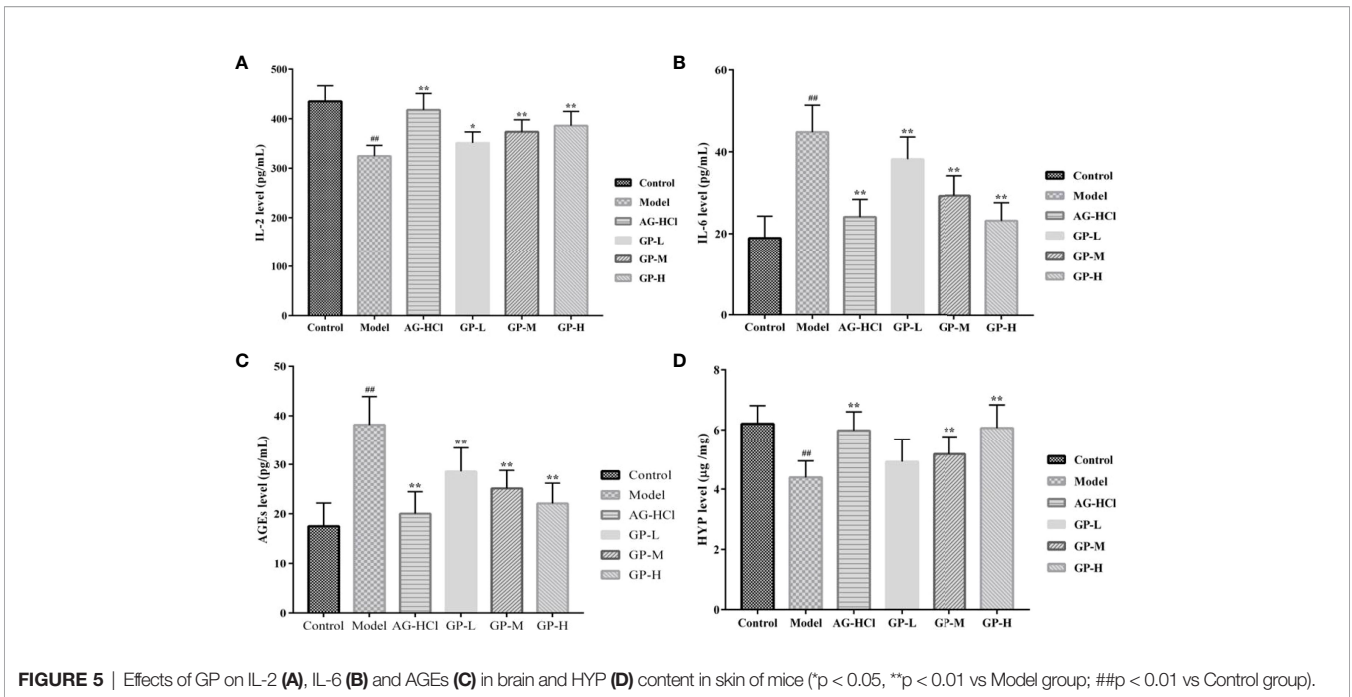

FIGURE 4 | Effects of GP on SOD **(A)**, GSH-Px **(B)**, CAT **(C)**, and MDA **(D)** in brain of mice (*p < 0.05, **p < 0.01 vs Model group; ##p < 0.01 vs Control group).

the control group (**Figure 5**). Treatment with GP could markedly decrease AGE levels in direct correlation to the dose ($P < 0.01$). It can provide a theoretical basis for its application in delaying brain aging and preventing neurodegenerative diseases, such as Alzheimer's disease and Parkinson's disease.

As the signature amino acid in the collagen sequence, hydroxyproline could be measured conveniently to monitor the contents of collagen and its fragments (Gu et al., 2020). The hydroxyproline content in the D-galactose group was significantly lower compared with the control group ($P < 0.01$; **Figure 5**), whereas the administration of GP significantly reversed the reduction of the hydroxyproline content in a dose-dependent manner ($P < 0.01$). With continuous growth of the body with aging, the solubility of collagen in skin decreases, but the degree of cross-linking increases.

FIGURE 5 | Effects of GP on IL-2 **(A)**, IL-6 **(B)** and AGEs **(C)** in brain and HYP **(D)** content in skin of mice (*p < 0.05, **p < 0.01 vs Model group; ##p < 0.01 vs Control group).
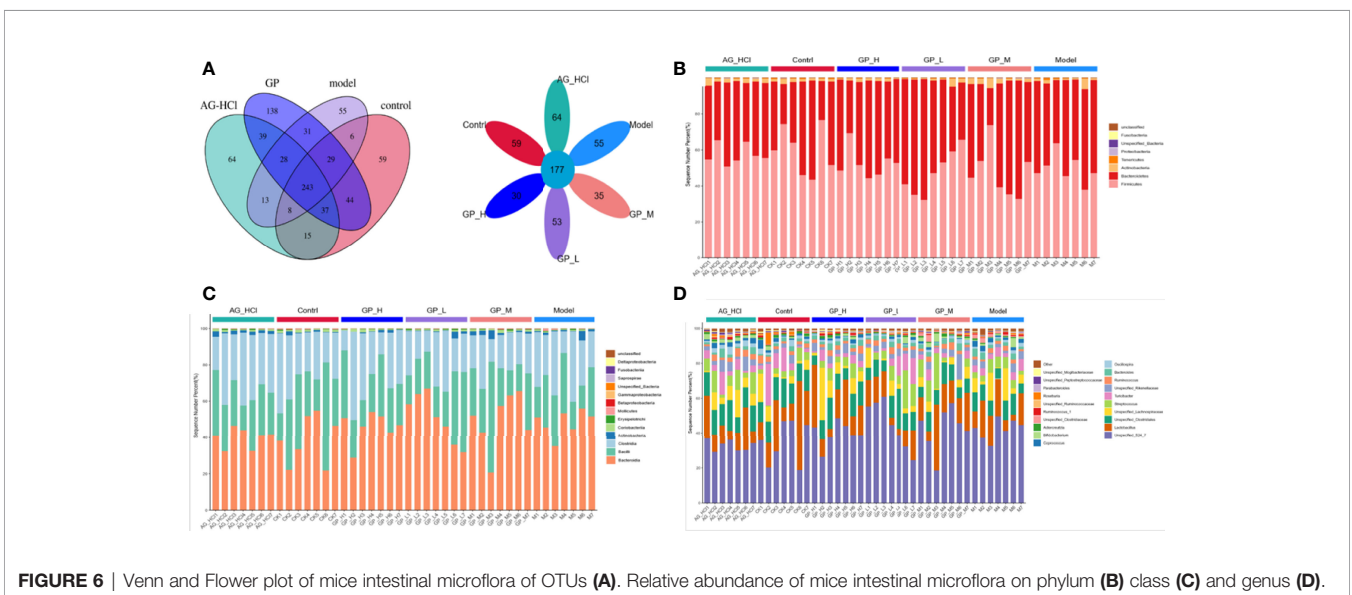
As a result, the hydroxyproline content and permeability of skin tissue decrease, whereas visible wrinkles increase significantly. Thus, GP played a role in inhibiting skin aging.

Sequence Analysis of the Intestinal Flora

The Veen figure visually showed the common and specific operational taxonomic unit (OTU) quantities (**Figure 6A**). There were 177 OTUs in all groups and 118 OTUs in GP groups, showing a 33% difference between GP and other groups. Changes in the intestinal flora were investigated using the 16*S* ribosomal RNA gene sequence analysis. A total of eight phyla were detected, including Firmicutes, Bacteroidetes, Actinobacteria, tenerictes, and proteobacteria (**Figure 6B**). On average, >96.98% of all samples comprised Firmicutes and Bacteroidetes. Under normal circumstances, Firmicutes and Bacteroidetes dominate in the intestine, and the Firmicutes/Bacteroidetes ratio is an important index for the degree of intestinal flora disorders. It is also closely related to changes in the body mass index (Quagliariello et al., 2016). In the medium-dose GP group, Firmicutes and Bacteroidetes accounted for 47.57% and 49.41%, respectively. The Firmicutes/Bacteroidetes ratios were 0.96 and 1.03 in the medium-dose GP and D-galactose groups, respectively.

FIGURE 6 | Venn and Flower plot of mice intestinal microflora of OTUs **(A)**. Relative abundance of mice intestinal microflora on phylum **(B)** class **(C)** and genus **(D)**.

Further in-depth excavation and analysis of mice intestinal flora at the levels of class and genus could more clearly show the trend of changes in beneficial and harmful bacteria in each component of the mouse intestinal tract. *Unspecified_S24_7* was dominant (>30%) in all groups (**Figure 6**). The abundance of *Bacillus* in the D-galactose group was the lowest (23.12%), whereas that in the GP group did not differ significantly from the positive control group (25.83% and 25.72%, respectively). Furthermore, the relative abundance change in *Clostridia* spp. was obvious in the GP group. The relative abundance of

Lactobacillus spp. increased to 17.41% and 17.46% in the medium- and high-dose subgroups of the GP group, respectively, showing significant changes compared with the D-galactose group (13.93%). *Lactobacillus* spp. are microorganisms beneficial to the health of the host, which can ferment sugars to produce lactic acid, maintain the health of animals, and regulate immune function (Heeney et al., 2017). Moreover, GP in the feed also significantly affected the relative abundance of other genera, including *Clostridium*, *Lachnospira*, and *Ruminococcus*, which are probiotics.
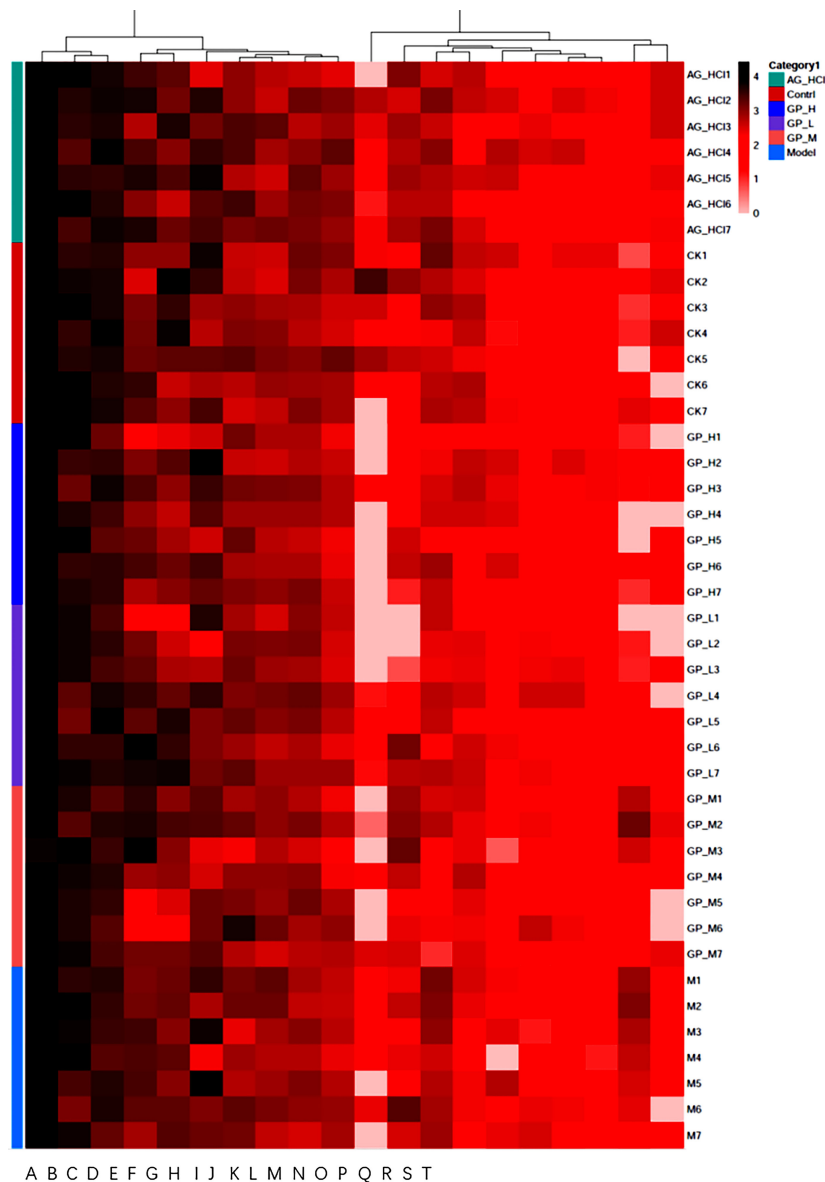

FIGURE 7 | The heatmap on genus **(A)** Unspecified_S24_7; **(B)** Lactobacillus; **(C)** Unspecified_Clostridiales; **(D)** Streptococcus; **(E)** Turicibacter; **(F)** Unspecified _Lachnospiraceae; **(G)** Unspecified_Rikenellaceae; **(H)** Bacteroides; **(I)** Ruminococcus; **(J)** Oscillospira; **(K)** Roseburia; **(L)** Bifidobacterium; **(M)** Coprococcus); **(N)** Adlercreutzia; **(O)** Ruminococcus; **(P)** Parabacteroides; **(Q)** Unspecified_Ruminococcaceae; **(R)** Unspecified_Mogibacteriaceae; **(S)** Unspecified_Clostridiaceae; **(T)** Unspecified_Peptostreptococcaceae.

OTU Difference Significance Analysis

LefSe identified differences in the individual taxa abundance. The control group showed predominance of Firmicutes and Bacteroidetes. The relative abundances of *Bifidobacterium*, Bifidobacteriales, Bifidobacteriaceae, *Actinobacteria*, *Clostridium*, Erysipelotrichales, Erysipelotrichi, and Erysipelotrichaceae were higher in the GP group (**Figure 7**). *Bifidobacteria* inhibit the excessive reproduction of harmful bacteria in the intestine by hydrolyzing bile acids into free bile acids and releasing synthetic H_2O_2, extracellular glycosidase, protein similar to bacteriocin, and other metabolites, to maintain the abundance of dominant bacteria in the intestine and improve the intestinal mucosal barrier (Turroni et al., 2022). The results indicated that the intestinal flora was significantly altered after GP treatment, and GP could alleviate dysbiosis by restoring the structure and diversity of the intestinal flora. Spearman correlation heatmap was constructed to determine any potential correlation in intestinal flora compositions. Compared with the control group, *Roseburia* and *Unspecified_Pepto streptococcaceae* in the GP group decreased significantly (**Figure 8**). We found that GP significantly reduced the abundance of harmful bacteria in the intestinal tract of mice.

Alpha and Beta Diversities

Shannon indices show the richness and evenness of species and reflect the species diversity in a community. Complexity of a sample is directly proportional to Shannon index. **Figure 9A** shows the analysis of the intestinal microbial alpha diversity of the rainbow trout in different test groups. Compared with the control group, community richness of the high-dose GP group was significantly higher ($P < 0.05$). Thus, the addition of GP significantly changed the intestinal microbial diversity of the rainbow trout.

Figures 9B, C show the analysis of beta diversity of intestinal microbiota of the rainbow trout in different groups. Three GP groups were clustered into one category, and the control and model groups were separated, indicating that D-galactose caused significant alterations in the beta diversity of the intestinal flora and microbial population distributions of GP groups were significantly different from the control and D-galactose groups. The partial least-squares discriminant analysis showed that the intestinal flora of the GP group was significantly different from the D-galactose group.

Intestinal flora disorders are a manifestation and cause of GP, showing mainly an increase in conditionally pathogenic bacteria and a decrease in beneficial bacteria compared with the healthy population. This study showed that GP alone elevated the abundances of nine OTUs (*Bacteroidales_S24-7*, *Lactobacillus*, *Lachnospira*, *Ruminococcus*, etc.). Among them, *Lachnospira* and *Ruminococcus* have certain intestinal protective effects. The abundance of these two kinds of bacteria changed significantly in gastrointestinal inflammation-induced model mice. *Bacteroidales_S24-7* can degrade polysaccharide substrates in the intestine, including plant hemicellulose and pectin, glycoproteins secreted by the host, and glycoproteins secreted by microorganisms α-Dextran (Wang et al.,
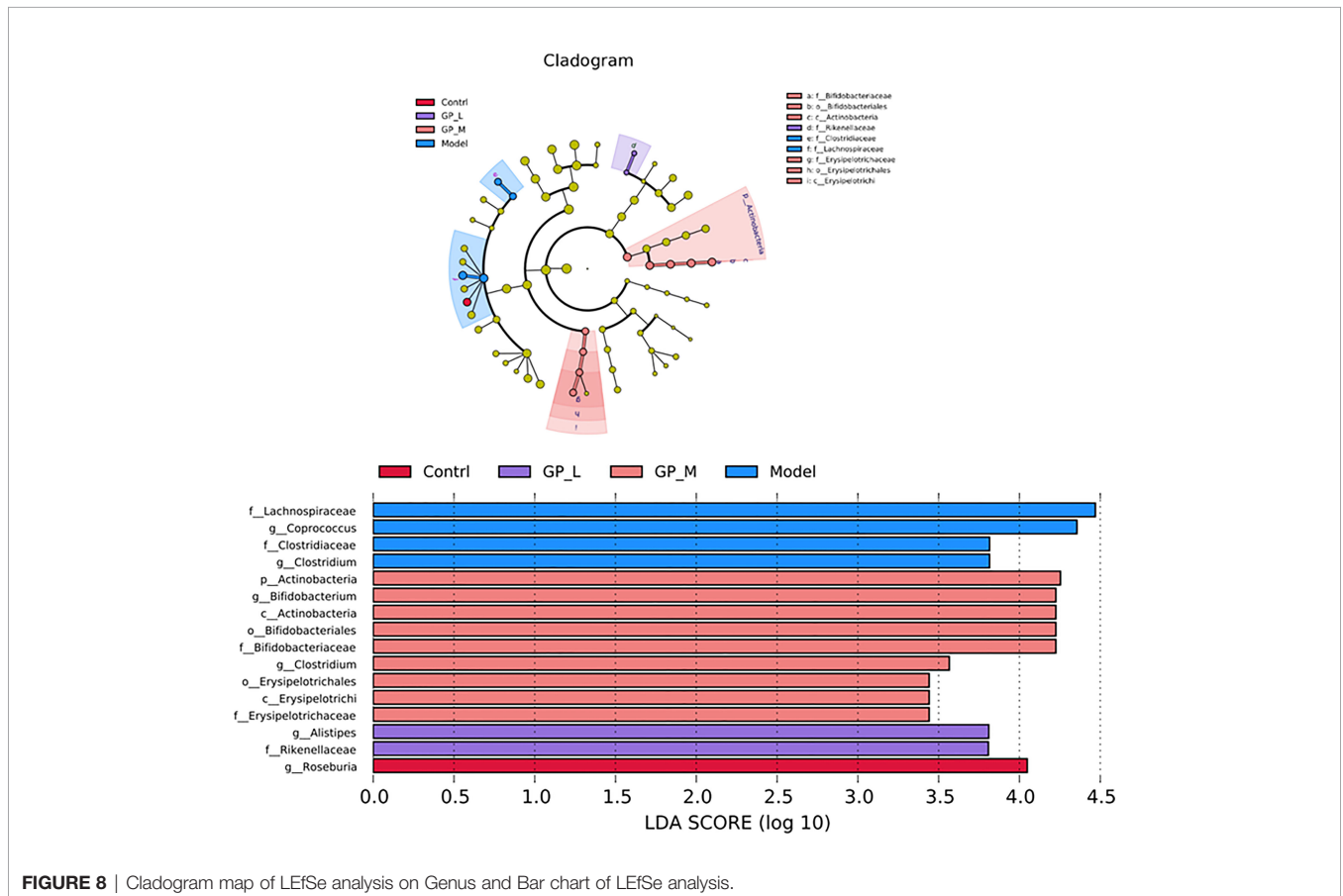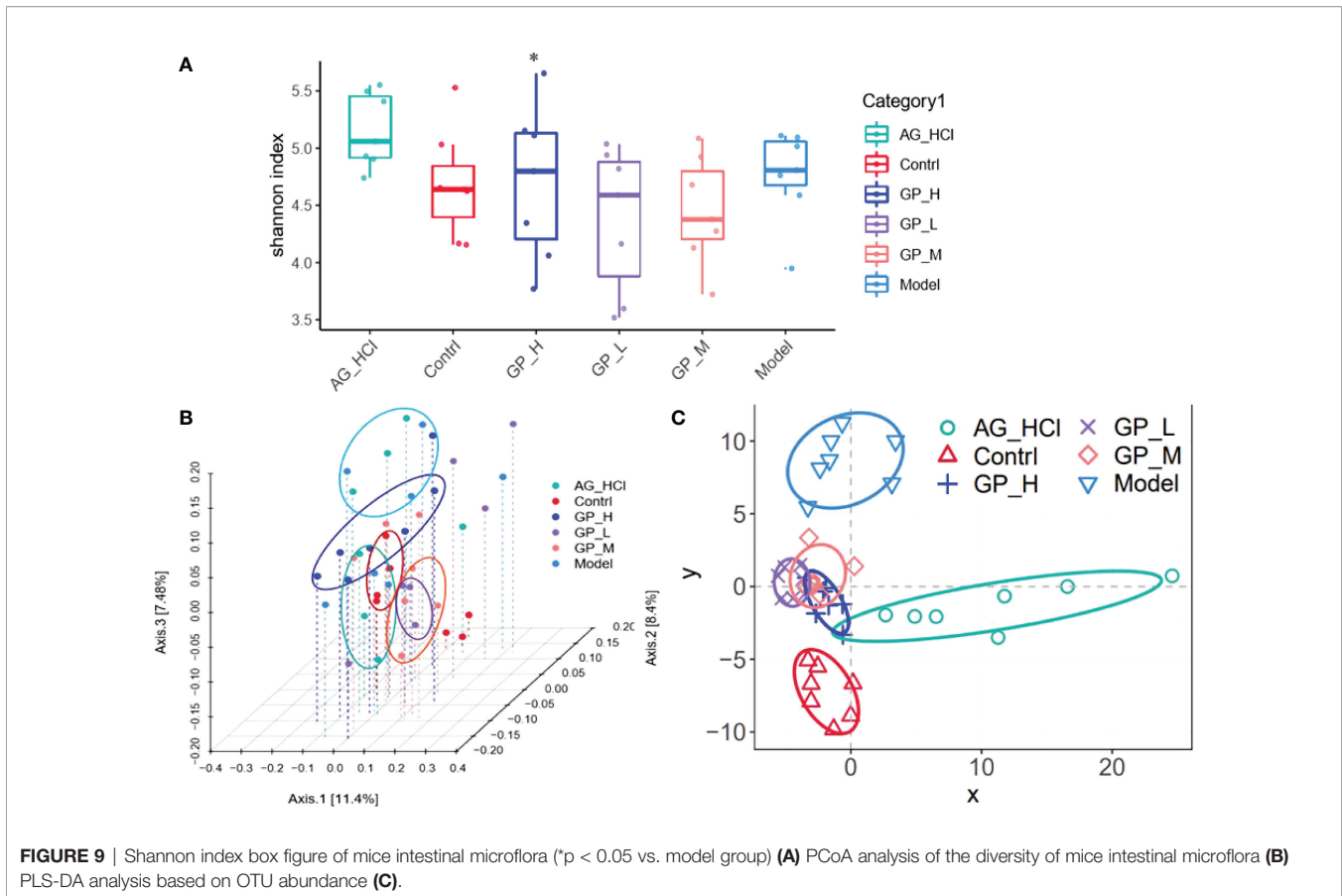

FIGURE 8 | Cladogram map of LEfSe analysis on Genus and Bar chart of LEfSe analysis.

FIGURE 9 | Shannon index box figure of mice intestinal microflora (*p < 0.05 vs. model group) **(A)** PCoA analysis of the diversity of mice intestinal microflora **(B)** PLS-DA analysis based on OTU abundance **(C)**.

2022). Simultaneously, some members of *S24-7* participate in the labeling and differentiation of active immune IgA, which plays an important role in maintaining the balance of the intestinal microecological community. Thus, GP significantly improved disorders of the intestinal flora in D-galactose–induced aging mice.

CONCLUSION

GP, a polysaccharide isolated from *G. lemaneiformi*, could significantly ameliorate age-related behavior and cognitive deficit in D-galactose–treated mice. It regulated intestinal bacteria, changed serum metabolite composition, and improved oxidative stress ability and inflammation. It improved the composition and structure of the intestinal microbiota in aging mice and increased *Lactobacillus*, *Bacteroides*, and *Akkermansia* spp. to a certain extent, which maintained intestinal balance and stability. Furthermore, it has the potential to become a functional food supplement in the near future to delay aging.

DATA AVAILABILITY STATEMENT

The datasets presented in this study can be found in online repositories. The names of the repository/repositories and accession number(s) can be found below: NCBI, PRJNA836043.

ETHICS STATEMENT

The animal study was reviewed and approved by Ethics Committee of experimental animal welfare and ethics committee of Huzhou University.

AUTHOR CONTRIBUTIONS

Writing—original draft preparation: ZZ; conceptualization: XW; validation: XX; data curation: GM; resources: XS; investigation: ZZ and NX; writing—review and editing: ZZ and NX. All authors contributed to the article and approved the submitted version.

FUNDING

REFERENCES

Baynes, J. W. (2001). The Role of AGEs in Aging Causation or Correlation. *Exp. Gerontol.* 36, 1527–1537. doi: 10.1016/S0531-5565(01)00138-3

Borgoni, S., Kudryashova, K. S., Burka, K., and Magalhães, J. P. (2021). Targeting Immune Dysfunction in Aging. *Ageing Res. Rev.* 70, 101410. doi: 10.1016/j.arr.2021.101410

Cui, X., Zuo, P. P., Zhang, Q., Li, X. K., Hu, Y. Z., Long, J. G., et al. (2006). Chronic Systemic D-Galactose Exposure Induces Memory Loss, Neurodegeneration, and Oxidative Damage in Mice: Protective Effects of R-α-Lipoic Acid. *J. Neurosci. Res.* 83, 1584–1590. doi: 10.1002/jnr.20845

Forman, H. J. (2016). Redox Signaling: An Evolution From Free Radicals to Aging. *Free Radic. Biol. Med.* 97, 398–407. doi: 10.1016/j.freeradbiomed.2016.07.003

Galkin, F., Zhang, B. H., Dmitriev, S. E., and Gladyshev, V. N. (2019). Reversibility of Irreversible Aging. *Ageing Res. Rev.* 49, 104–114. doi: 10.1016/j.arr.2018.11.008

García-Pea, C., Álvarez-Cisneros, T., Quiroz-Baez, R., and Friedland, R. P. (2017). Microbiota and Aging. A Review and Commentary. *Arch. Med. Res.* 48, 681–689. doi: 10.1016/j.arcmed.2017.11.005

Gu, Y. P., Han, J. X., Jiang, C. P., and Zhang, Y. (2020). Biomarkers, Oxidative Stress and Autophagy in Skin Aging. *Ageing Res. Rev.* 59, 101036. doi: 10.1016/j.arr.2020.101036

Heeney, D. D., Gareau, M. G., and Marco, M. L. (2017). Intestinal *Lactobacillus* in Health and Disease, a Driver or Just Along for the Ride? *Curr. Opin. Biotechnol.* 49, 140–147. doi: 10.1016/j.copbio.2017.08.004

Ionescu-Tucker, A., and Cotman, C. W. (2021). Emerging Roles of Oxidative Stress in Brain Aging and Alzheimer's Disease. *Neurobiol. Aging* 107, 86–95. doi: 10.1016/j.neurobiolaging.2021.07.014

Lakshminarayanan, B., Stanton, C., O'Toole, P. W., and Ross, R. P. (2014). Compositional Dynamics of the Human Intestinal Microbiota With Aging: Implications for Health. *J. Nutr. Health Aging* 18, 773–786. doi: 10.1007/s12603-014-0549-6

Quagliariello, A., Aloisio, I., Cionci, N. B., Luiselli, D., D'Auria, G., Martinez-Priego, L., et al. (2016). Effect of *Bifidobacterium Breve* on the Intestinal Microbiota of Coeliac Children on a Gluten Free Diet: A Pilot Study. *Nutrients* 8, 660–675. doi: 10.3390/nu8100660

Rehman, S. U., Shah, S. A., Ali, T., Chung, J. I., and Kim, M. O. (2017). Anthocyanins Reversed D-Galactose-Induced Oxidative Stress and Neuroinflammation Mediated Cognitive Impairment in Adult Rats. *Mol. Neurobiol.* 54, 255–271. doi: 10.1007/s12035-015-9604-5

Sendama, W. (2020). The Effect of Ageing on the Resolution of Inflammation. *Ageing Res. Rev.* 57, 101000. doi: 10.1016/j.arr.2019.101000

Turroni, F., Milani, C., Ventura, M., and Sinderen, D. (2022). The Human Gut Microbiota During the Initial Stages of Life: Insights From Bifidobacteria. *Curr. Opin. Biotechnol.* 73, 81–87. doi: 10.1016/j.copbio.2021.07.012

Vlassara, H. (1997). Recent Progress in Advanced Glycation End Products and Diabetic Complications. *Diabetes* 46, S19–S25. doi: 10.2337/diab.46.2.S19

Wang, L., Wang, Y. W., Zhang, P., Song, C., Pan, F., Li, G., et al. (2022). Gut Microbiota Changes in Patients With Spondyloarthritis: A Systematic Review. *Semin. Arthritis Rheum.* 52, 151925. doi: 10.1016/j.semarthrit.2021.11.002

Wang, X. M., Zhang, Z. S., Wu, Y., Sun, X., and Xu, N. J. (2018). Synthesized Sulfated and Acetylated Derivatives of Polysaccharide Extracted From *Gracilariopsis Lemaneiformis* and Their Potential Antioxidant and Immunological Activity. *Int. J. Biol. Macromol.* 124, 568–572. doi: 10.1016/j.ijbiomac.2018.11.244

Wang, X. M., Zhang, Z. S., Zhang, S. Y., Yang, F., Yang, M., Zhou, J. B., et al. (2021). Antiaging Compounds From Marine Organisms. *Food Res. Int.* 143, 110313. doi: 10.1016/j.foodres.2021.110313

Wang, X. M., Zhang, Z. S., Zhou, H. C., Sun, X., and Xu, N. J. (2019). The Anti-Aging Effects of *Gracilaria Lemaneiformis* Polysaccharide in *Caenorhabditis Elegans*. *Int. J. Biol. Macromol.* 140, 600–604. doi: 10.1016/j.ijbiomac.2019.08.186

Xu, L. Q., Xie, Y. L., Gui, S. H., Zhang, X., Mo, Z. Z., Sun, C. Y., et al. (2016). Polydatin Attenuates D-Galactose-Induced Liver and Brain Damage Through its Anti-Oxidative, Anti-Inflammatory and Anti-Apoptotic Effects in Mice. *Food Func.* 7, 4545–4555. doi: 10.1039/C6FO01057A

Yosri, N., Khalifa, S. A. M., Guo, Z. M., Xu, B., Zou, X. B., and EI-Seedi, H. R. (2021). Marine Organisms: Pioneer Natural Sources of Polysaccharides/Proteins for Green Synthesis of Nanoparticles and Their Potential Applications. *Int. J. Biol. Macromol.* 193, 1767–1798. doi: 10.1016/j.ijbiomac.2021.10.229

Zhang, Z. S., Wang, X. M., Han, S. W., Liu, C. B., and Liu, F. (2018). Effect of Two Seaweed Polysaccharides on Intestinal Microbiota in Mice Evaluated by Illumina PE250 Sequencing. *Int. J. Biol. Macromol.* 112, 796–802. doi: 10.1016/j.ijbiomac.2018.01.192